OMTM, Volume *10*

Supplemental Information

Bioengineered Viral Platform for Intramuscular Passive Vaccine Delivery to Human Skeletal Muscle

Nicole K. Paulk, Katja Pekrun, Gregory W. Charville, Katie Maguire-Nguyen, Michael N. Wosczyna, Jianpeng Xu, Yue Zhang, Leszek Lisowski, Bryan Yoo, Jose G. Vilches-Moure, Gordon K. Lee, Joseph B. Shrager, Thomas A. Rando, and Mark A. Kay

SUPPLEMENTAL FIGURES:

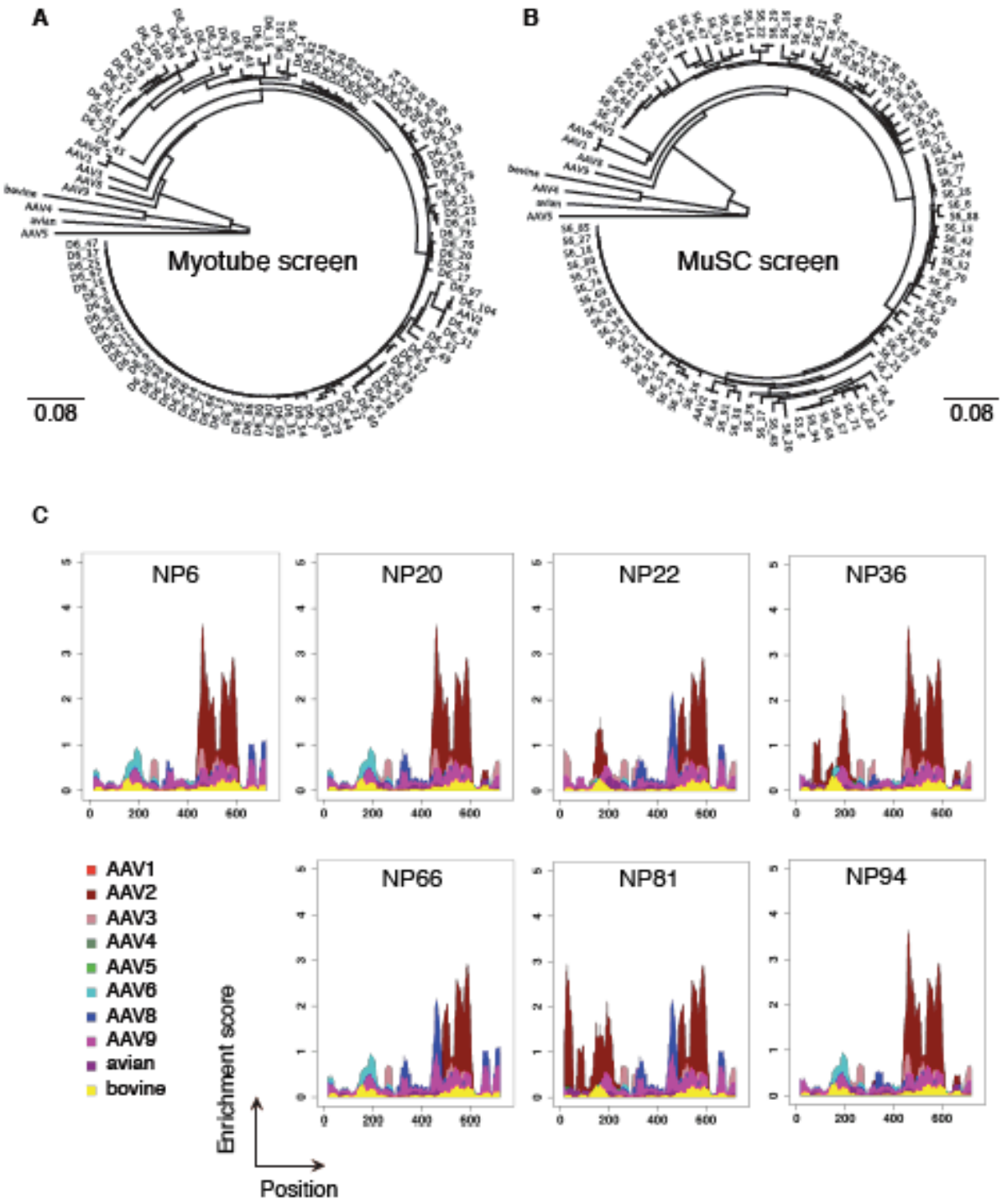

Figure S1: Phylogeny and enrichment scores of top capsid variants from completion of each screen. **(A)** Phylogenetic tree showing genetic relatedness at the amino acid level among the parental serotypes in the library and the top 100 selected variants from round six of the screen in differentiated human myotubes pooled from five patients. **(B)** Phylogenetic tree showing genetic relatedness at the amino acid level among the parental serotypes in the library and the top 100 selected variants from round six of the screen in primary human skeletal muscle stem cells pooled from five patients. **(C)** Enrichment scores were calculated for each amino acid position in the sequence of each chimera by comparison of sequences from parental serotypes based on maximum likelihood. Library parents are depicted in different colors as shown.

A

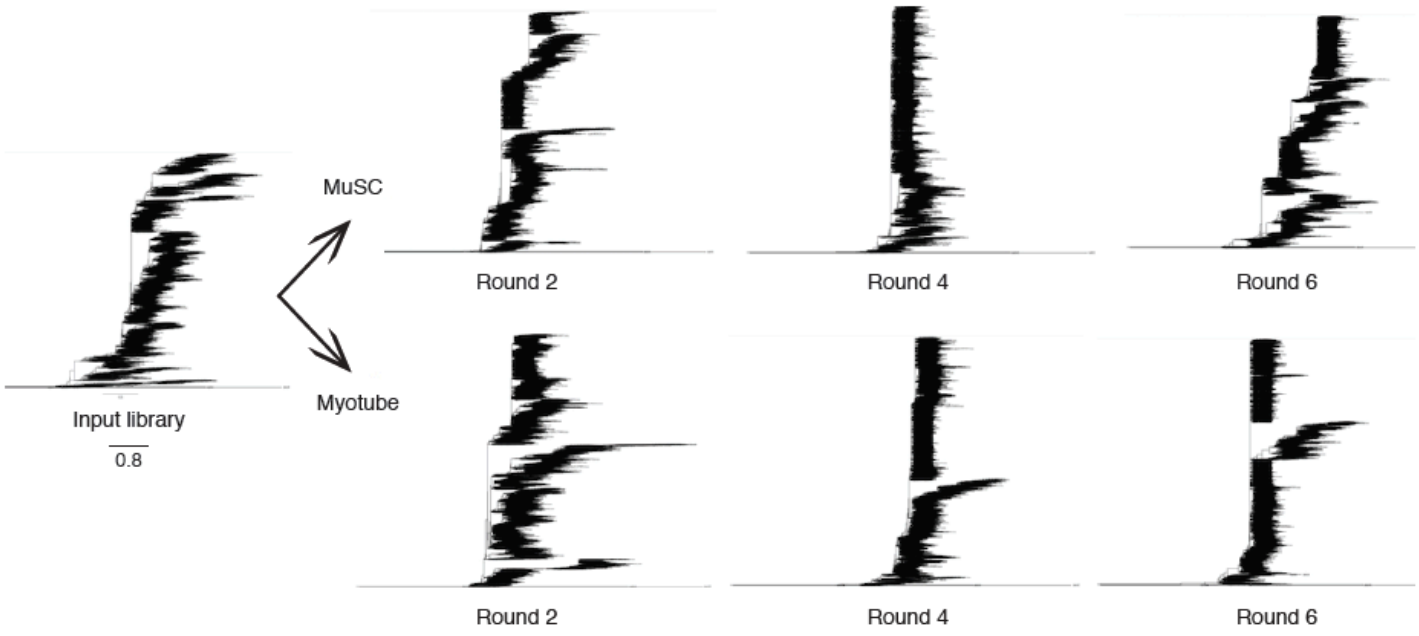

B

Round	Raw CCS reads	CCS reads post-filtering
Input library	30,910	13,845
Round 2 MuSC	6,410	3,898
Round 4 MuSC	6,345	3,302
Round 6 MuSC	18,369	11,085
Round 2 Myotube	14,343	7,612
Round 4 Myotube	10,645	6,569
Round 6 Myotube	19,542	12,724

Figure S2: Round-by-round phylogenetic trees of all variants by PacBio single molecule sequencing.
(A) Comparative phylogenies showing genetic relatedness at the amino acid level among the parental serotypes in the library and all library variants. The decreasing diversity and increasing enrichment going from the unselected AAV library through rounds 2, 4 and 6 for each screen (human MuSC and myotube) are shown. **(B)** Raw and filtered CCS read counts used to generate panel (A) are shown.

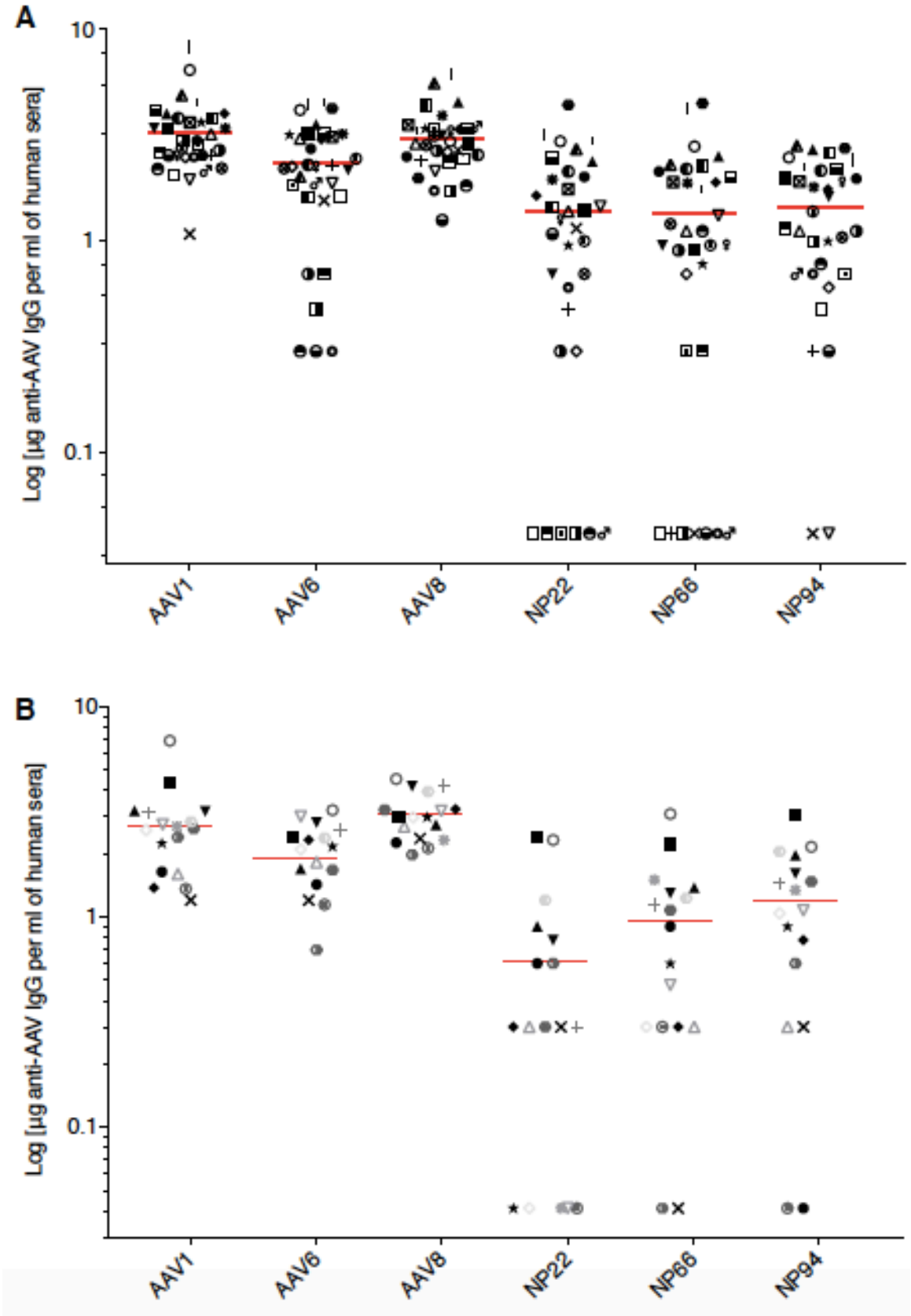

Figure S3: Seroreactivity profiling by patient sex.
Seroreactivity ELISA assay for presence of anti-AAV antibodies in normal human serum from 50 US adults. (**A**) Male patients. (**B**) Female patients. Each patient was assayed in technical triplicates with data points representing the mean minus background. Symbols are consistent across treatments for each patient to allow comparisons.

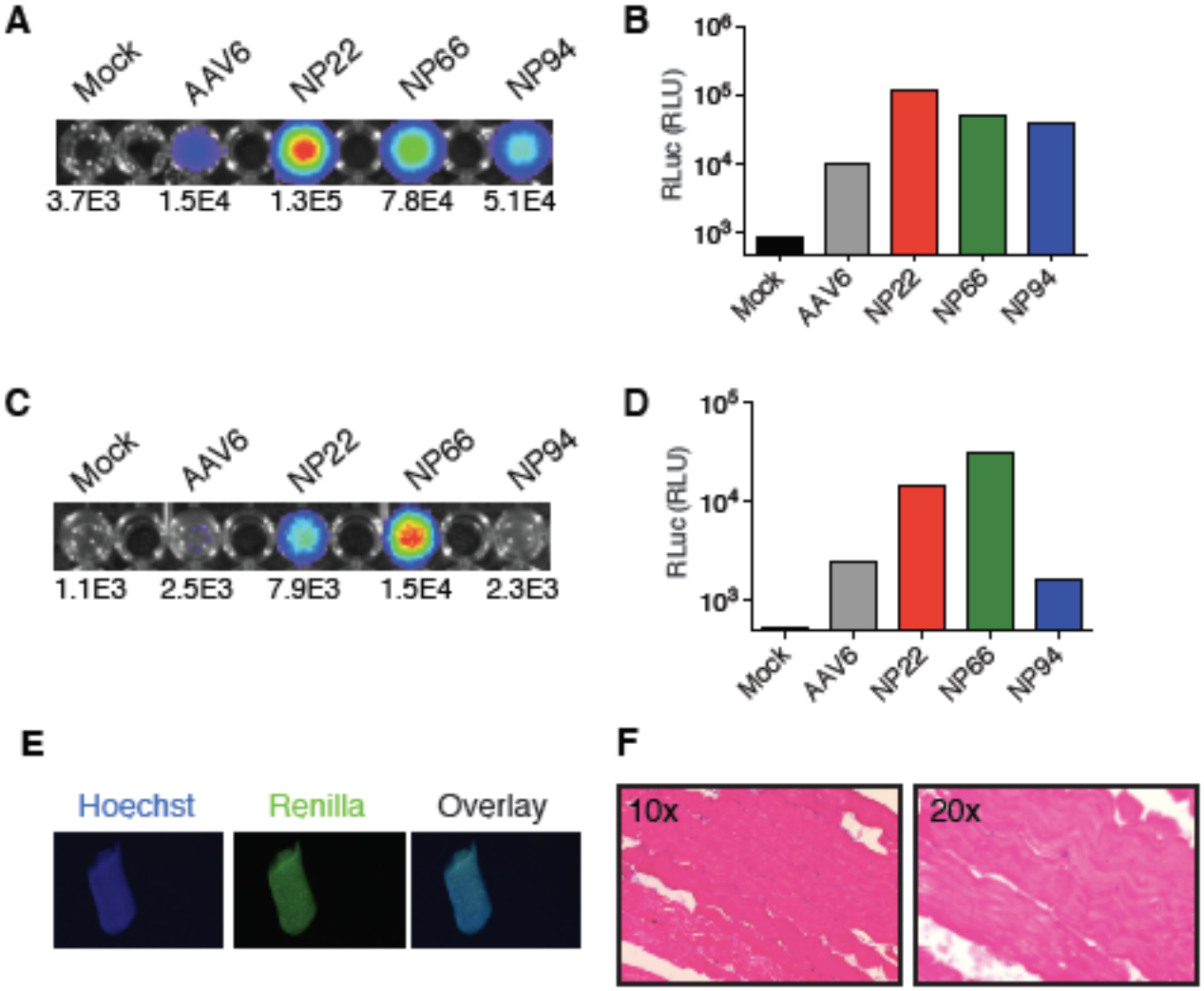

Figure S4: Additional *ex vivo* data support superior transduction with new shuffled variants.
(**A**) RLuc imaging at 48-hrs on 1 replicate (due to small muscle sample size) of human *rectus abdominis* muscle fibers transduced with PBS, rAAV6, NP22 or NP66 expressing scAAV-CAG-RLuc *ex vivo*. Radiance (p/s/cm^2/sr) displayed below each treatment. **(B)** RLuc assay on lysed *r. abdominis* fibers at 48-hrs post-transduction. **(C)** RLuc imaging on 1 replicate (due to small muscle sample size) of human *latissimus dorsi* fibers transduced with PBS, rAAV6, NP22 or NP66 expressing scAAV-CAG-RLuc *ex vivo*. **(D)** RLuc assay on lysed *l. dorsi* fibers at 48-hrs post-transduction. Radiance displayed below each treatment. (**E**) Representative staining of transduced single human *l. dorsi* muscle fibers for RLuc (green) and Hoechst (blue) from patient-4 at 40X magnification demonstrating viral uptake along entire fiber length. (**F**) H&E stains of rhesus *b. femoris* muscle at 10X and 20X magnification demonstrating normal skeletal muscle architecture.

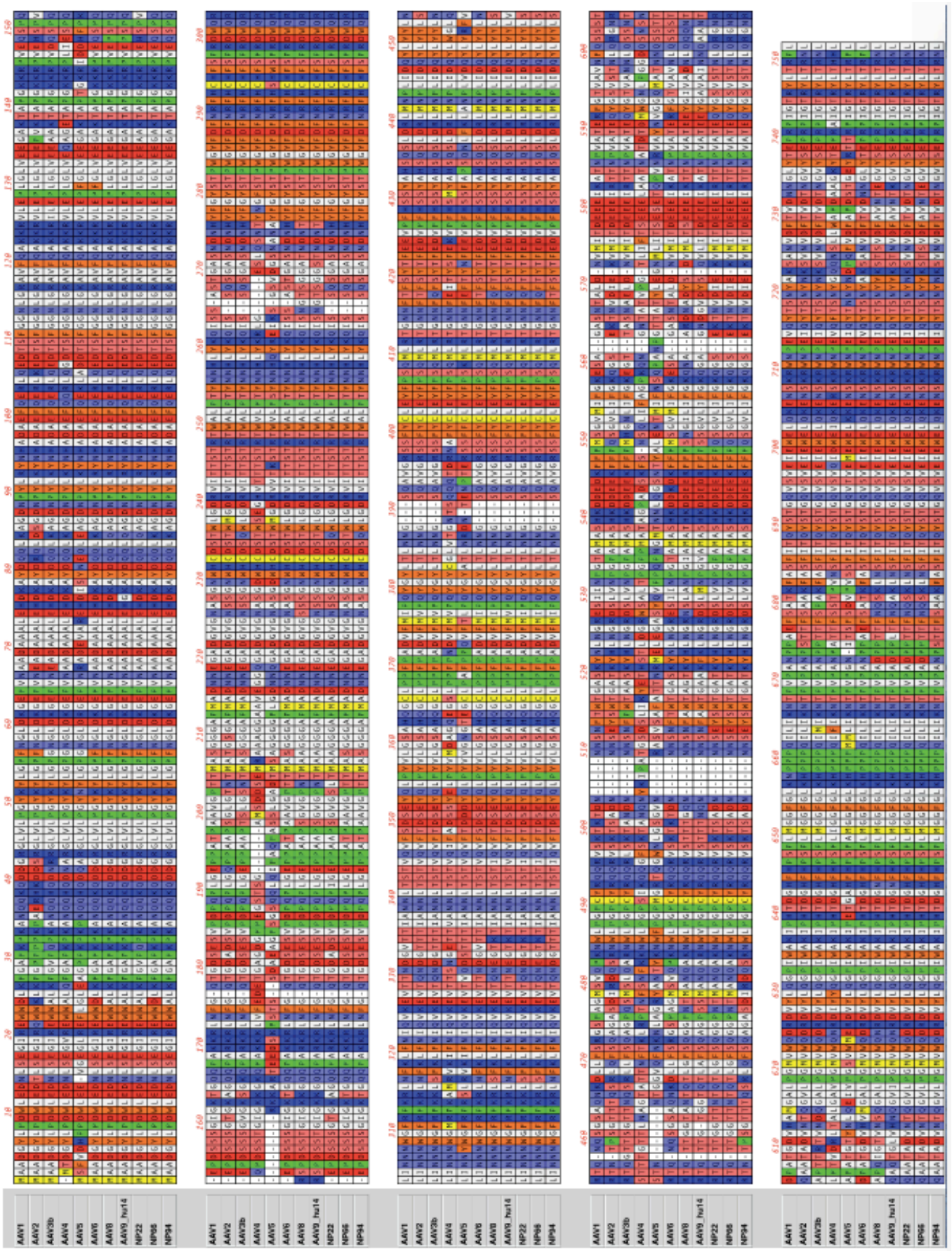

Figure S5: Amino acid sequences of best performing shuffled capsid variants.
Comparative amino acid sequence alignments of shuffled AAV variants to the parental serotypes.

SUPPLEMENTAL TABLES

Table S1: Details for normal off-clot human serum samples. Details on 50 adult U.S. serum donors including date of sample blood draw (DOS), age at time of donation, sex, ethnicity, smoker status and ABO blood type. All donors were negative for HBV, HCV and HIV (data not shown).

DOS	Age	Sex	Ethnicity	Smoke	ABO		DOS	Age	Sex	Ethnicity	Smoke	ABO
1/29/16	34	Male	Black	Yes	B+		1/29/16	55	Male	Black	Yes	A+
2/8/16	23	Female	Caucasian	Yes	O+		1/29/16	22	Male	Black	Yes	O+
2/8/16	37	Female	Black	No	A+		1/29/16	52	Male	Black	Yes	B+
2/8/16	21	Female	Black	No	O+		1/29/16	22	Male	Black	No	A+
2/8/16	37	Female	Caucasian	Yes	A-		1/29/16	24	Male	Black	Yes	A+
2/8/16	24	Female	Caucasian	No	A-		2/5/16	18	Female	Black	Yes	A+
1/29/16	21	Male	Black	No	O+		1/29/16	40	Male	Black	No	B+
1/29/16	23	Male	Black	Yes	O+		1/29/16	33	Male	Black	Yes	A+
1/29/16	25	Female	Black	Yes	O+		1/12/16	42	Male	Black	No	B+
1/29/16	25	Male	Black	Yes	O+		1/29/16	22	Male	Black	No	O+
2/5/16	27	Female	Black	No	A+		1/29/16	22	Female	Black	No	A+
1/29/16	21	Male	Black	Yes	B+		1/29/16	41	Male	Caucasian	Yes	A-
2/8/16	21	Female	Black	Yes	O+		1/29/16	23	Male	Black	Yes	O+
1/29/16	20	Male	Black	Yes	O+		1/12/16	39	Male	Caucasian	Yes	A-
1/12/16	31	Male	Black	Yes	A+		1/29/16	18	Male	Black	No	O+
1/29/16	29	Male	Black	No	B+		1/29/16	19	Male	Black	Yes	O+
1/29/16	42	Male	Black	Yes	A+		1/29/16	23	Female	Black	No	O+
1/29/16	20	Male	Black	Yes	O+		1/29/16	18	Female	Black	No	A+
1/29/16	39	Female	Black	Yes	B+		1/29/16	42	Male	Black	Yes	A+
1/29/16	30	Male	Black	Yes	B+		1/29/16	24	Male	Black	Yes	O+
1/29/16	22	Male	Black	Yes	A+		1/29/16	53	Male	Black	Yes	A+
1/29/16	35	Male	Black	Yes	A+		1/12/16	24	Male	Black	No	B+
1/29/16	24	Male	Black	No	A+		1/29/16	59	Female	Black	Yes	B+
2/5/16	18	Female	Caucasian	No	O+		1/29/16	22	Female	Black	Yes	O+
2/5/16	36	Female	Black	No	B+		1/29/16	43	Male	Black	No	A+

Table S2: Known functional motif conservation across shuffled and parental capsid serotypes.
AA = amino acid; PLA2 = phospholipase 2; HSPG = heparin sulfate proteoglycan; SA = sialic acid. Note, AAV9 is version hu14, and VP1 numbering is used. For SA and HSPG binding, parental serotypes with gray shaded boxes indicate serotypes which have the indicated function. Corresponding shaded boxes in the evolved variants indicate that they evolved a residue at that position from one of the parents with either SA or HSPG binding functions.

AA position	Attributed function	1	2	3b	4	5	6	8	9	NP22	NP66	NP94
129	In PLA2 domain	L	L	L	L	F	F	L	L	L	L	L
418	Post-entry transduction	E	D	D	K	E	D	D	D	D	D	D
447	SA binding	N	S	N	Q	V	N	S	V	S	S	S
472	SA binding	S	R	S	S	A	S	A	A	A	A	R
473	SA binding	V	D	L	N	N	V	N	N	N	N	D
485	HSPG binding	R	R	R	K	R	R	R	R	R	R	R
488	HSPG binding	R	R	R	G	G	R	R	R	R	R	R
500	SA binding	N	E	N	D	V	N	N	N	E	E	E
502	SA binding	T	S	P	L	A	T	A	A	S	S	S
503	SA binding	W	W	W	I	F	W	W	W	W	W	W
528	Receptor attachment	K	K	K	G	L	K	K	K	K	K	K
531	HSPG binding/transduction	E	E	E	D	S	K	E	E	E	E	E
533	HSPG binding	K	K	K	K	N	K	R	R	K	K	K
584	Receptor attachment	F	L	L	D	N	L	L	N	L	L	L
586	HSPG binding	S	R	S	S	S	S	Q	A	R	R	R
589	HSPG binding	T	R	T	N	T	T	T	T	R	R	R
642	Post-entry transduction	N	H	H	H	H	H	H	H	H	H	H

Table S3: Different amino acids between evolved variants NP22, NP66 and NP94.
AA = amino acid position with VP1 numbering. Orientation prediction is based on the available crystal structure residues for AAV8 (amino acid positions prior to 220 are uncharacterized in existing structures). Shaded boxes in gray highlight differences between the three capsid variants.

AA position	Predicted orientation	NP22	NP66	NP94
24	n/a	A	D	A
29	n/a	V	A	A
31	n/a	Q	K	K
84	n/a	Q	K	K
135	n/a	A	G	G
148	n/a	H	Q	Q
151	n/a	V	Q	Q
159	n/a	T	I	I
162	n/a	A	T	T
168	n/a	R	K	K
179	n/a	A	S	S
180	n/a	D	E	E
188	n/a	I	L	L
194	n/a	A	T	T
196	n/a	S	A	A
197	n/a	G	A	A
200	n/a	S	P	P
201	n/a	L	T	T
205	n/a	A	S	S
224	Internal	S	A	A
233	Internal	Q	T	Q
310	Internal	K	R	R
312	Internal	S	N	N
327	External (top of cylinder)	D	E	D
330	External (base of cylinder)	K	K	T
410	Internal	Q	Q	T
412	Internal	T	T	S
449	External (base of 3-fold protrusion)	Q	Q	N
451	Internal	T	T	P
452	External (on 3-fold protrusion)	G	G	S
456	External (on 3-fold protrusion)	N	N	T
457	External (on 3-fold protrusion)	T	T	Q
458	External (on 3-fold protrusion)	Q	Q	S
459	External (on 3-fold protrusion)	T	T	R
461	External (on 3-fold protrusion)	G	G	Q
465	External (base of 3-fold protrusion)	G	G	A
467	External (base of 3-fold protrusion)	P	P	A
468	Internal	N	N	S
469	External (base of 3-fold protrusion)	T	T	D
470	External (base of 3-fold protrusion)	M	M	I
471	External (base of 3-fold protrusion)	A	A	R
472	External (base of 3-fold protrusion)	N	N	D
474	External (base of 3-fold protrusion)	A	A	S
475	External (base of 3-fold protrusion)	K	K	R
656	Internal	D	D	N
658	External (base of cylinder)	P	P	S
662	External (canyon)	N	N	S
663	External (canyon)	Q	Q	A
664	External (canyon)	S	S	A
666	External (canyon)	L	L	F
667	External (canyon)	N	N	A
705	External (base of 3-fold protrusion)	N	Y	N
708	External (base of 3-fold protrusion)	V	T	V
709	External (on 3-fold protrusion)	N	S	N
713	External (base of 3-fold protrusion)	T	A	T
715	External (canyon)	D	N	D